Voltage-based Non-Standard Inverse Time for Over Current Relay in Distribution System connected DFIG-based Wind Turbines

N. Ha-upala and K. Bhumkittipich*

Abstract*— *The penetration of the distributed generation-based wind turbine on the distribution system affects the fault clearing time of the protective relay and mal-operation of the protective relay coordination. This paper presented a new voltage-based nonstandard time current characteristic. The development of the nonstandard characteristic was based on the electromechanical induction disc relay equation. The proposed nonstandard characteristic relay model was implemented on the radial distribution system connected to DFIG-based wind turbines. The fulfillment of this research is the reduced total clearing time of the protection scheme by using the proposed voltage-based nonstandard characteristic relay. The fast tripping of the proposed nonstandard characteristic relay maintained the connection of the wind turbine generators with the distribution system during a fault. This is the achievement of the low voltage ride through capability enhancement to the wind turbine generation by the modified protective relay characteristic.

***Keywords*— DFIG-based wind turbine, nonstandard characteristic, time coordination, overcurrent relay, fast tripping, low voltage ride through.**

1. INTRODUCTION

The number of wind turbine generations (WTG) connected to the distribution system (DS) is increasing every year. WTG connections reduce the distribution system impedance. This leads to the high short circuit current [1]-[2]. According to the grid code, the wind turbine generation must remain on the grid connection during a fault on the grid side [3]-[5]. This condition changes the short circuit current magnitude and direction due to the current feed from WTG. The alteration of short circuit current characteristic creates mal-operation on the overcurrent relay. Fig. 1 shows an example of this problem. When a fault occurs at point F1, the operation of relay R3 is tripping for the fault clearing and R2 is tripping according to R3 due to the fault current through R2 increased by the feeding current from WTG, while the tripping time of R1 increases because the current through R1 decreases. This is incoordination between R1, R2 and R3. Sympathetic tripping can occur on R1 because the fault current supplying through R1 from WTG and R1 is a bidirectional overcurrent relay [6]-[11].

Improvement of the incoordination and sympathy tripping for protective relay uses the nonstandard characteristic. The nonstandard characteristics are created by considering the conventional relay characteristic, electrical magnitudes, fault characteristics, admittance of transmission line and coordination between protective devices[12]-[18]. In [12], the methodology of nonstandard characteristic creation is classified as:

- Including electrical quantity
- Standard characteristic combination
- Arithmetical function approach

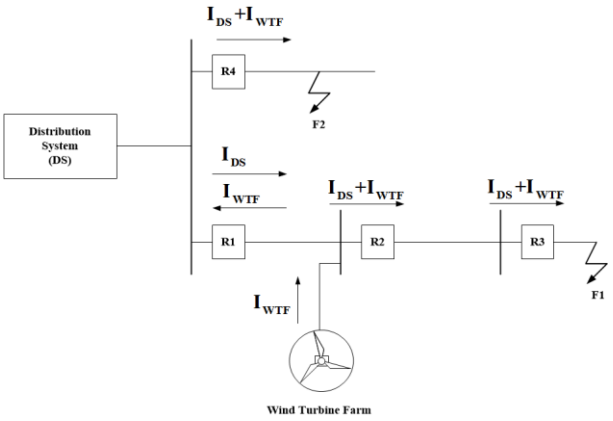

Fig. 1. Example of the mal-operation problem of the protection relay.

The entire methodology generated the complex equation form. Some parameters of the equation are difficult for determination. The nonstandard characteristic can be applied on the protection scheme by programming the nonstandard equation to the microprocessor based on a protective device such as a protective relay and re-closer [19]-[20]. The coordination of nonstandard characteristics based on a protective device in the distribution system is a challenging problem for researchers. The optimal tripping time solution such as nonlinear programing (NLP), genetic algorithm (GA), particle swarm optimization (PSO) is the popular method for the time coordinate determination

N. Ha-upala is with Power and Energy System Research Center, Department of Electrical Engineering, Faculty of Engineering, Rajamangala University of Technology Thanyaburi (RMUTT), Pathum Thani, Thailand.

K. Bhumkittipich is with Power and Energy System Research Center, Department of Electrical Engineering, Faculty of Engineering, Rajamangala University of Technology Thanyaburi (RMUTT), Pathum Thani, Thailand.

*Corresponding author: K. Bhumkittipich; Phone: +66-2-549-3571; Fax: +66-2-549-3422; E-mail: krischonme.b@en.rmutt.ac.th.

of the nonstandard characteristic relay [20]-[24].

The voltage-based nonstandard inverse time-current characteristic is a nonstandard characteristic considering voltage magnitude. This characteristic is constantly evolving for application on the microprocessor-based overcurrent relay. The voltage-based nonstandard characteristic equation generally includes the logarithm function. This results in the complexity of the equation and challenge for the application [12]. This paper presents a new voltage-based nonstandard time current characteristic for the microprocessor-based relay. The development of nonstandard characteristic is based on the electromechanical induction disc relay equation. The nonstandard characteristic equation combines the voltage magnitude with current magnitude for the operating time determination. The aims of the proposed characteristic include fault clearing by the minimum tripping time and the improvement of the relay tripping time fluctuation due to the effect of fault current feeding for the distribution system connected with the DFIG based wind turbine generation. In this paper, a new voltage-based nonstandard characteristic relay is applied on the free communication protection scheme for the radial system connected with wind turbine generator protection. The simulation changes the fault point, the location and the sizing of WTG. The result of the simulation is a comparison of three operating time characteristics comprising the proposed nonstandard characteristic, the voltage nonstandard characteristic and the standard characteristic. The discussion and conclusion present the advantages of the proposed nonstandard characteristic considering the low voltage ride-through capability of the WTG.

2. STANDARD AND VOLTAGE-BASED NONSTANDARD CHARACTERISTICS

The standard inverse time-current characteristic as the IEC60255-3 standard [25] is produced based on the induction disc motion characteristic. The ratio of input current to the pickup current is related to the disc driving torque. It is represented in terms of current multiplier (*M*). The influence of the damper and the spring torque is represented as *A* constant and the exponent value (*B*) is dependent on the inverse time-current curve shape. The operating time of the standard equation varies by the changing of the time multiplier setting (TMS). The standard equation is shown as Eq.1.

$$t = \frac{A}{M^B - 1} \times TMS \tag{1}$$

The saturation flux of the induction disc is due to the multiple of current magnitude produced the operating time constant. For this result, the time-current equation of IEEE C37.112-1996 standard [26] includes the C parameter. Equation 2 shows the inverse-time current according to IEEE standard.

$$t = \left[\frac{A}{M^B - 1} + C \right] \times TMS \tag{2}$$

Operating time according to Eq.1 and Eq.2 is dependent on the current magnitude and *TMS*. The changing of *TMS* in Eq.1 and Eq.2 affects the time coordination of both characteristic equations.

Currently, the penetration of distributed generation on the distribution system is influenced by the fault current magnitude and voltage magnitude. This affects the protective device coordination. The protection system engineer proved the problem of coordination by using the voltage-based nonstandard characteristics relay. The first voltage-based nonstandard time-current equation as Eq.3 introduced by [22]-[23]. The characteristic of Eq.3 is applied to the directional overcurrent relay for the distribution system with the wind turbine farm connection. This application proposed fast tripping by voltage controlled for the fault clearing considering the low voltage ride-through capability time. The determination of the optimum factor *K* and *TMS* is the coordination problem solution of the characteristic equation 3.

$$t = \left(\frac{1}{e^{1-v_f}} \right)^k \left(\frac{A}{M^B - 1} \right) \times TMS \tag{3}$$

In [19]-[20], the combination between the voltage-based nonstandard current-time characteristic with the standard inverse time-current characteristic as equation 4 and equation 5 applied to the re-closer characteristic for the prevention of the fuse blowing due to the transient current. Equation 4 is a combination between the voltage-based nonstandard characteristic with the IEC60255-3 standard inverse time-current characteristic and a combination between the voltage-based nonstandard current-time characteristic with the IEEE extremely inverse time standard characteristic, as shown in equation 5. Parameter *K* of Eq.4 and Eq.5 depends on the voltage magnitude according to the fault type. The coordination problem of the characteristic in equation 4 and equation 5 is the determination of the optimal parameter *K* and *TMS*.

$$t = \left(\frac{A}{M^B - 1} \right) \left(\frac{V_f}{e^{kVf}} \right) \times TMS \tag{4}$$

$$t = \left[\frac{28.2}{M^2 - \left(\frac{1}{e^{1-Vf}} \right)^2} + 0.127 \right] \times (1 - V_f) V_f \times TMS \tag{5}$$

Equation 6 is an example of the natural logarithm function based on the nonstandard characteristic equation. This nonstandard characteristic equation applied to the microprocessor is based on the relay for non-communication protection scheme of the distribution system connected with the synchronous based distributed generation [27]. The optimal time coordination problem of equation 6 is the computation of the optimal parameter *K* and *TMS*.

$$t = TMS \times \left(\frac{V_f^K}{e^{Vf}} \right) \times \left[\frac{A}{\left(\ln\left(V_n \frac{I_f}{V_f} \right) \right)^p - \left(\ln\left(V_n \frac{I_f}{V_f} \right) \right)^p} + B \right] + D \quad (6)$$

During a fault on the distribution system connected inverter-based distribution generator, the high fault current suddenly fed to the fault location. The logarithm function based nonstandard equation (as Eq.7) was applied to the microprocessor based relay for instantaneously tripping to the fault clearing. The determination of the optimum *TMS* solved the time coordination problem for Eq.7 [28].

$$t = \left[\frac{A}{M^B - 1} \right] \left(\frac{1}{1 - \log_V^k} \right)^Z \times TMS \quad (7)$$

The creation of a nonstandard characteristic by the logarithm curve fitting method [29] obtained the logarithm based nonstandard characteristic equation, as Equation 8. This equation applied to the protective relay for the distribution system connected the synchronous based distributed generation [30].

$$t = \frac{\log(V_f + A)}{M^B - 1} + C \quad (8)$$

The fault on the loop based connection system of the wind farm caused the different voltage magnitude on the connecting point of the wind turbine and the fault current feeding in two directions. This led to all wind turbines being disconnected from the loop system. In [31], the voltage-based nonstandard overcurrent relay applied for the fault clearing on the loop system. The characteristic equation of the relay is shown in Eq.9. This equation reduced the operating time of Eq.9 that can be reduced by multiplying the saturate time constants (*C*) with the fault voltage ratio.

$$t = \left(\frac{A}{M^2 - 1} + C\left(\frac{V_f}{V_{rate}} \right) \right) \times TMS \quad (9)$$

The application of the voltage-based nonstandard time current characteristics on the protection scheme for the minimized fault clearing time is the solution for the protection problem of the distribution system connecting the distributed generation. The time coordination problem of the voltage-based nonstandard characteristic equation is the determination of the optimal parameter for the characteristic equation. The optimal solution as nonlinear programming (NLP), genetic algorithm (GA) and particle swarm optimization (PSO) is the general method for finding a solution to the time coordination problem. The complex form of the nonstandard characteristic equation was challenging for the protection system researcher.

3. NEW VOLTAGE-BASED NONSTANDARD TIME-CURRENT CHARACTERISTIC

The new voltage-based, nonstandard time current characteristic is a development based on the induction disc relay equation. In [26][32], the induction disc rotating equation can be presented as:

$$K_I I^2 = K_d \frac{d\theta}{dt} + \tau_S \quad (9)$$

where, I is the measuring current; θ is the disc rotating angle; τ_S is the spring torque; K_I is a relating current to torque constant; K_d is a damping constant.

The driving torque of an induction disc in Eq. (9) is related to the voltage magnitude and current magnitude. Therefore, the disc rotating equation can be presented as:

$$K_V V K_I I^2 = K_d \frac{d\theta}{dt} + \tau_S \quad (10)$$

The $K_V V$ is the driving torque of voltage magnitude. The torque of voltage magnitude is related to the ratio of input voltage to the pickup voltage and the torque of current is related to the ratio of input fault current to the pickup current. Then, equation (10) can be solved by replacing $V = V_P M_V$ and $I = I_P M_I$. The solution for Eq. (11) is obtained as:

$$t = \frac{A}{M_V^D M_I^B - 1} \times TMS \quad (11)$$

where, M_I is the pickup current multiplier; M_V is the pickup voltage multiplier; *D* is the exponent constant dependent on the input voltage magnitude; *B* is the exponent constant dependent on the conventional standard characteristic; *A* is the ratio of damping factor to the initial spring torque.

The influence of voltage magnitude to the new nonstandard characteristic is shown as a graph in Fig 2. The equation (12) sets the constant *A=13.5* and *B*=1 as the very inverse time standard characteristic IEC60255-3. The voltage multiplier (M_V) is (1-*V*)/(1-V_P). *V* is the per/unit input voltage and the pickup voltage (V_P) is setting between 0.05-0.95. The magnitude voltage factor *D* equals 1. The graph shows the relation for the operating time of the relay with the current multiplier by changing the input voltage. The decreasing of voltage magnitude reduced the tripping time.

Parameter *D* is the exponent factor of the voltage multiplier. The changing value of *D* affects the slope of the characteristic curve. This influences the coordination of the relay. The value of D can be varied between 0 and 1. If D=0, the input voltage does not affect the characteristic curve. The influence of D factor on the characteristic curve is shown in Fig. 3.

The selection value of D factor must be considered for the principle of relay coordination. In this paper, it is defined that the D factor depends on the per-unit input voltage magnitude by setting the D factor as D= V_{nom}-*V*. The effect of parameter D to the time-voltage is shown in Fig.4. The operating time constants at the D=0. When D=V_{nom}-*V*, the operating time is decreased to the minimum value at *V*=1. The slope of the curve is nonlinear at D=1.

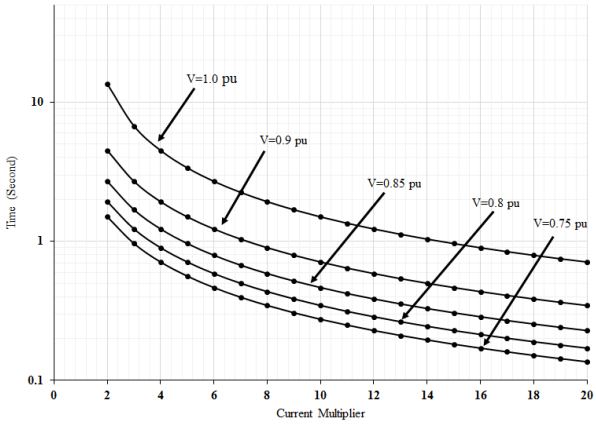

Fig. 2. Influence of the voltage magnitude on time-current characteristic.

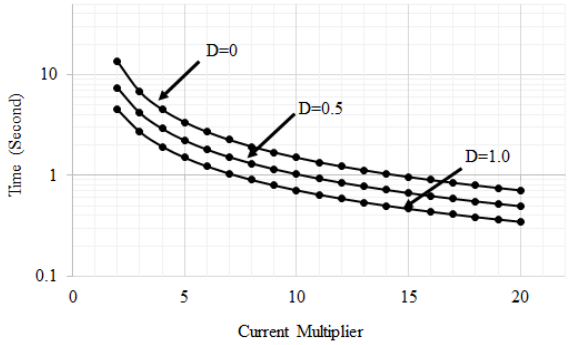

Fig. 3. Influence of parameter D on the time-current characteristic.

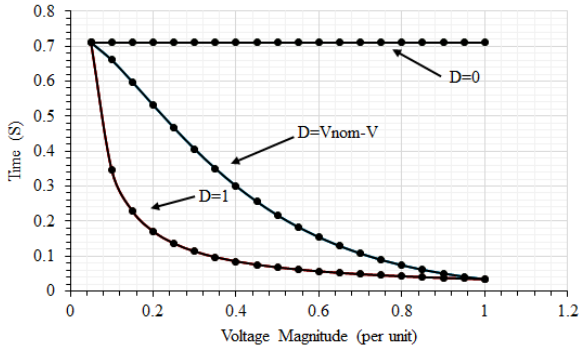

Fig.4. Effect of parameter D on operating time.

4. SIMULATION DETAILS AND SETUP

The simulation is classified into two parts: the characteristic equation testing and the operation testing. The characteristic testing determines the relationship between the multiplier current with the operating time of the proposed nonstandard characteristic and compared with the conventional standard characteristic (Eq.1) and the voltage-based nonstandard characteristic (Eq.2). Three characteristic equations set the parameters of time-current function as the very inverse time characteristic. Parameter K of Eq.2 equals 2 and the input voltage constant at 0.05pu. The pickup voltage (V_P) of the proposed equation sets 0.05per unit.

The operation testing tests three relay models: model 1 is the conventional standard relay, model 2 is the voltage-based nonstandard relay, and model 3 is the proposed nonstandard relay. All models are simulated by using the MATLAB program. The 33kV radial distribution system consists of three bus and the 10MW load connection at bus 3 as Fig.5. The simulation is classified into five scenarios. The first scenario is the radial distribution system without the wind turbine generator. The scenario 2 is the installation of 10MW DFIG-based wind turbine generator with the radial system on bus 2. The scenario 3 is the replacement of the 10MW wind turbine generator by the 20MW wind turbine generator on bus 2. The location of wind turbine generator changed from bus2 into bus 3 in the scenario 4, and the sizing of the wind turbine generator at bus 3 is increased to 20MW in Scenario 5. All scenarios applied the three phase fault and changed the fault location in order to bus1, bus2 and bus3. The setting parameters of three relay are shown in Table 1. Three relay models operate in the instantaneous mode when the tripping time is less than 0.01 sec.

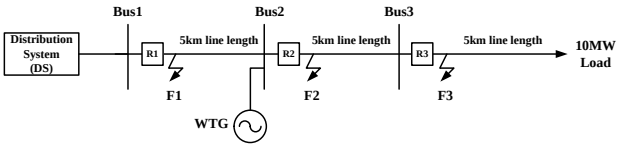

Fig.5. The 3-bus radial system of the operation testing.

5. SIMULATION RESULTS AND DISCUSSION

5.1 Characteristic equation testing

The results of three characteristics equation relay testing are shown in Fig. 6. The graph compared three characteristics of relays. The conventional standard relay is the operating time higher than two nonstandard relay. The proposed nonstandard relay is the lowest tripping time compared to the voltage-based nonstandard relay. Three characteristic testing is based on the TMS=1.

Table 1. Setting parameters of the relay model

Location	Pickup Current (A)	TMS		
		Model 1 relay	Model 2 relay	Model 3 relay
Bus 1	700	0.111	0.096	0.059
Bus 2	500	0.095	0.33	0.394
Bus 3	500	0.05	0.05	0.088

5.2 The operation testing

The results of simulations are classified according to 5 scenarios. Each result for the simulations discusses the operation of the proposed nonstandard overcurrent relay in each scenario. The operation of the proposed overcurrent relay is compared with the conventional standard overcurrent relay and the voltage-based overcurrent relay.

Scenario 1: The result according Table 1, the fault applied on bus1 causes the instantaneous tripping of the primary relay due to the fault location being nearest to

the distribution system. The proposed nonstandard overcurrent relay in three fault location is faster tripping than the conventional characteristic relay and the nonstandard characteristic relay. The total clearing time of proposed nonstandard overcurrent relay is decreased by 42.17% of the voltage-based nonstandard relay and 54.65% of the conventional standard relay.

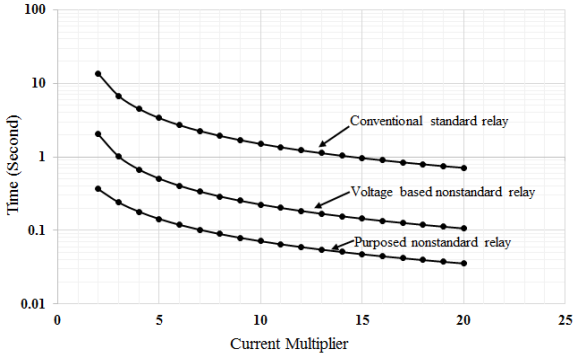

Fig. 6. Comparison of three characteristic based on TMS=1.

Table 2. Result of three relay operations for scenario 1

Fault Location	Operating Time (s)		
	Model 1 relay	Model 2 relay	Model 3 relay
Bus 1	R_{p1}:0.01	R_{p1}:0.01	R_{p1}:0.01
Bus 2	R_{p2}:0.356	R_{p2}:0.169	R_{p2}:0.169
	R_{b1}:0.656	R_{b1}:0.591	R_{b1}:0.358
Bus 3	R_{p3}:0.332	R_{p3}:0.045	R_{p3}:0.02
	R_{b2}:0.632	R_{b2}:0.592	R_{b2}:0.32
	R_{b1}:1.290	R_{b1}:1.162	R_{b1}:0.709
Total Time (s)	3.277	2.570	1.486
R_p: Primary relay		R_b: Primary relay	

Table 3. Result of three relay operations for scenario 2

Fault Location	Operating Time (s)		
	Model 1 relay	Model 2 relay	Model 3 relay
Bus 1	R_{p1}:0.01	R_{p1}:0.01	R_{p1}:0.01
Bus 2	R_{p2}:0.259	R_{p2}:0.123	R_{p2}:0.045
	R_{b1}:0.668	R_{b1}:0.602	R_{b1}:0.365
Bus 3	R_{p3}:0.268	R_{p3}:0.036	R_{p3}:0.0172
	R_{b2}:0.510	R_{b2}:0.512	R_{b2}:0.310
	R_{b1}:1.515	R_{b1}:1.366	R_{b1}:0.835
Total Time (s)	3.233	2.651	1.583
R_p: Primary relay		R_b: Primary relay	

Scenario 2: The connection of 10MW wind turbine at bus2 and fault applying on bus 1, 2 and 3, the primary relay of the proposed nonstandard characteristic has lower total operating time than 51.03% of the conventional standard relay and 40.28% of the nonstandard relay.

When the fault is on bus3, the backup relay of the proposed nonstandard characteristic shows a slight increase in the operating time compared to the voltage-based nonstandard characteristic relay. This causes the current feeding from the wind turbine generator. This affects the voltage multiplier and current multiplier of the proposed nonstandard relay. The result is shown in Table 3.

Scenario 3: The increasing capacity of the wind turbine generator up to 20MW connected with a radial system at bus2 and fault simulation on bus1, 2 and 3, the fault current feeding from wind turbine during fault on bus 3 causes voltage sag magnitude not related to the short circuit current level on bus 2. This affects the backup protection of the proposed nonstandard characteristic relay. For this scenario, the total fault clearing time for the proposed characteristic is reduced to 40.11% of the voltage-based nonstandard characteristic and 50.55% of the standard characteristic.

Table 4. Result of three relay operations for scenario 3

Fault Location	Operating Time (s)		
	Model 1 relay	Model 2 relay	Model 3 relay
Bus 1	R_{p1}:0.01	R_{p1}:0.01	R_{p1}:0.01
Bus 2	R_{p2}:0.310	R_{p2}:0.147	R_{p2}:0.052
	R_{b1}:0.712	R_{b1}:0.641	R_{b1}:0.389
Bus 3	R_{p3}:0.288	R_{p3}:0.039	R_{p3}:0.0181
	R_{b2}:0.549	R_{b2}:0.583	R_{b2}:0.362
	R_{b1}:1.616	R_{b1}:1.458	R_{b1}:0.786
Total Time (s)	3.487	2.879	1.724
R_p: Primary relay		R_b: Primary relay	

Scenario 4: The connection of the 10MW wind turbine on the bus 3. For the fault applied on bus 1, the proposed nonstandard relay on bus 3 is picked up due to the current feeding from the wind turbine generation to the fault location. For this scenario, the total operating time of the proposed nonstandard relay is decreased by 53.14% of the conventional standard relay and 42.19% of the voltage-based nonstandard relay.

Scenario 5: The changing of the wind turbine sizing up to 20MW and the fault applied on bus 1 result in the pickup on three types of relay on bus 2. This causes the current feeding increasing according the increasing of wind turbine generator capacity. The total operating time of the proposed nonstandard relay is reduced to 43.27% of the voltage-based nonstandard relay and 51.4% of the conventional standard relay.

Table 5. Result of three relay operations for scenario 4

Fault Location	Operating Time (s)		
	Model 1 relay	Model 2 relay	Model 3 relay
Bus 1	R_{p1}:0.01	R_{p1}:0.01	R_{p1}:0.01
Bus 2	R_{p2}:0.296	R_{p2}:0.140	R_{p2}:0.05
	R_{b1}:0.712	R_{b1}:0.641	R_{b1}:0.389
Bus 3	R_{p3}:0.282	R_{p3}:0.038	R_{p3}:0.0178
	R_{b2}:0.685	R_{b2}:0.649	R_{b2}:0.345
	R_{b1}:1.426	R_{b1}:1.286	R_{b1}:0.786
Total Time (s)	3.413	2.766	1.599
R_p: Primary relay		R_b: Primary relay	

Table 6. Result of three relay operations for scenario 5

Fault Location	Operating Time (s)		
	Model 1 relay	Model 2 relay	Model 3 relay
Bus 1	R_{p1}:0.01	R_{p1}:0.01	R_{p1}:0.01
Bus 2	R_{p2}:0.296	R_{p2}:0.140	R_{p2}:0.05
	R_{b1}:0.712	R_{b1}:0.641	R_{b1}:0.389
Bus 3	R_{p3}:0.147	R_{p3}:0.019	R_{p3}:0.010
	R_{b2}:0.685	R_{b2}:0.650	R_{b2}:0.346
	R_{b1}:1.426	R_{b1}:1.286	R_{b1}:0.786
Total Time (s)	3.278	2.739	1.593
R_p: Primary relay		R_b: Primary relay	

For the case of low voltage ride through capability enhancement is for the wind turbine generation. The voltage profile of wind turbines bus after tripping event of three models is shown in Fig. 7. The system setting as scenario 5, time applied fault at 0.5 s. The three models set the parameters of time-current function as the very inverse time characteristic and the TMS = 0.1. For this result, the tripping time of the conventional relay model (Model 1) is 0.759 s. while the peak voltage recovery is 1.135pu or 11.27% of the normal voltage. The nonstandard relay model (Model 2) trips the circuit breaker for the fault clearing at 0.54 s. After fault clearing, the peak recovery voltage is 1.134pu. and 11.17% of the normal voltage. For the operation of relay model 3, the proposed nonstandard characteristic relay clears the fault within 0.018 sec. The system voltage is recovered at 0.568 s and the peak recovery voltage is 1.068 or 4.7% of the nominal voltage.

The results of simulation for scenarios 1 to 5 indicate that the proposed voltage-based nonstandard characteristic can reduce the total operating time of the protection scheme. The fault clearing within the minimum time of the proposed nonstandard characteristic relay before the tripping of under voltage protection of the wind turbine farm is the increasing in the low voltage ride through capability for the wind turbine farm.

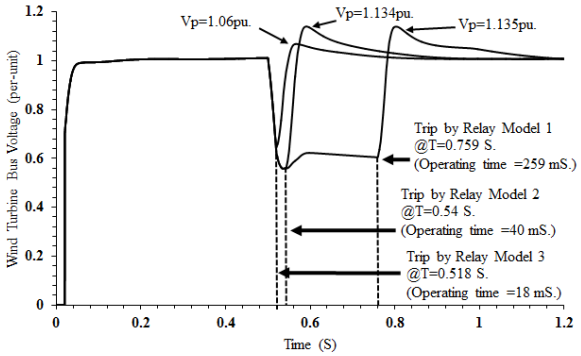

Fig.7. Wind turbine bus voltage profile after fault clearing.

The reducing of peak voltage recovery by the fast tripping of the proposed nonstandard characteristic relay can reduce the voltage oscillation and the effect of the peak of transient voltage to the insulation of electric device on the point common coupling. These are advantages of the new voltage-based nonstandard time-current characteristic.

6. CONCLUSION

This paper presents a new voltage-based nonstandard inverse time-current characteristic. The characteristic equation was created based on the dynamic equation of the induction disc relay. The inclusion of voltage magnitude means there is an increase in driving torque of the induction disc relay. The volume of the voltage multiplier varied according to voltage magnitude, pickup voltage and the parameter *D*. Parameter *D* of the characteristic can be set as a constant value between 0 to 1 or varying dependent on the voltage magnitude by $D=1-V$. The changing of parameter *D* affects the time coordination. The solution for the optimal time coordination problem of the proposed nonstandard equation is the determination of the optimum of *TMS* and *D*. For the results of simulation, the operating time characteristic was the lowest value at the minimum voltage magnitude and the operating time could control the voltage magnitude and parameter *D*. Achievement in the operation of the proposed nonstandard characteristic relay shows operation testing in five scenarios. The fast tripping of the proposed nonstandard characteristic relay reduces the total fault clearing time. Coordination between the primary relay with the backup relay based on the voltage magnitude was successful. The proposed nonstandard characteristics relay can trip very fast to the fault clearing on the distribution system connected the wind turbines farm. This maintained the connection of wind turbine farm with the distribution system during a fault on the grid side. This study enhanced the low voltage ride through capability to the wind turbine farm.

REFERENCES

[1] Yuan, H.; Guan, Z.; Kong, H.; and Zhang, B.H. 2015. Impact of Renewable Energy Integration on Overcurrent Protection in Distribution Network. In *The 27th Chinese Control and Decision Conference*. Qingdao, China, 23-25 May. DOI :10.1109/CCDC.2015.7162835

[2] Sa'ed, J.A.; Favuzza, S.; Ippolito, M.G.; Massaro, F. 2013. Verifying the effect of distributed generators on voltage profile, power losses and protection system in radial networks. In *4th International Conference on Power Engineering, Energy and Electrical Drives*. Istanbul Turkey, 13-17 May. DOI: https//doi.org/10.1016/j.jesit.2015.11.010

[3] Leao, R.P.S.; Almada,J.B.; Souza,P.A.;Cardoso, R.J.; Sampaio, R.F.; Lima, F.K.A.;Silveia, J.G.; and Formiga, L.E.P. 2010. The Implementation of the Low Voltgae-Ride Through Curve on the protection system of a wind power plant. *The 11th International Conference on Renewable Energies and Power Quality*. Spain, 13-15 April 2010. DOI: http://doi.org/10.24084/repqj09.635

[4] Xinyan,Z.; Xuan, C.;Weiqing,W. and Chao,Y. 2013. Fault ride-through study of wind turbines. *Journal of Power and Energy Engineering*,(1):25-29. DOI: http://dx.doi.org/10.4236/jpee.2013.15004

[5] Mali,S.;James,S. and Ishwari, T. 2014. Improving low voltage ride-through capabilities for grid connected wind turbine generator. *Energy Procedia* 54(2014):530-540.DOI: http://doi.org/10.1016/j.egypro.2014.07.294

[6] Mladenovic, S. and Azadvar, Ali A. 2010. Sympathetic trip prevent by applying simple current relay. In *IEEE PES General Meeting*. USA, 25-29 July 2010. DOI: 10.1109/PES.2010.5589955

[7] Kyle, J.; Cambell, B.; Martin, L. 2011. Analysis of the sympathetic tripping problem for network with high penetrations of distributed generation. In *International Conference on Advanced Power System Automation and Protection.* Beijing, China, 16-20 October 2011. DOI: 10.1109/APAP.2011.6180432.

[8] Kyle, J.; Campbell, B.; Coffele, F. and Rosoe A.J. Investigation of the sympathetic tripping problem in power systems with large penetrations of distributed generation. *IET Generation, Transmission & Distribution Vol.9*:379-385.

[9] Hussain, B.; Sarkh M.S.; Hussian, S.; and Abusara A.M. 2010. Integration of distributed generation into the grid: protection challenge and solutions. In *10th IET International Conference on Developments in Power System Protection*. Manchester, UK, 29March-1April. DOI: 10.1049/cp.2010.0347.

[10] Kennedy, J.; Ciufo, P. and Agalgaonkar, A. 2016. A review of protection system for distribution networks embedded with renewable generation. *Renewable and Sustainable Energy Reviews* 15 (2015):1308-1317.

[11] Vasileois, A.; George, N.; Vasilis A. and Nikos, D. 2017. Hardware-in-the-loop design and optimal setting of adaptive protection schemes for distribution system with distributed generation. *IEEE Transection on Power Delivery* 32(1):393-399.

[12] Hasan, C.; Ibrahim, S.; Huseyin, A.; Bedri, K.; Ozan, E. and Nikolaos, G. 2018. Power system protection with digital overcurrent relay: A review of non-standard characteristics. *Electrical Power System Research* 164(2018):89-102.

[13] Ritwik, M.; Manjula, D.; Arindam, G.; Gerard, L. and Firuz, Z. 2011. Control and protection of microgrid connected to utility through back-to-back converters. *Electrical Power System Research 81(2011)*:1424-1435.

[14] Manjula, D.; Ritwik, M.; Arindam, G. and Gerard, L. 2009. Converter and protection of microgrid with converter interfaced micro source. In *3rd International Conference on Power System*, Kharagpur, India, 27-29 December. DOI: 10.1109/ICPWS.2009.5442654.

[15] Dewadasa, M.; Ghosh, A. and Ledwich, G. 2009. Fold back current control and admittance protection scheme for a distribution network containing distributed generator. *IET Generation, Transmission & Distribution 4(8)*:952-962.

[16] Dewadasa, M.; Ghosh, A. and Ledwich. 2009. An inverse time admittance relay for fault detection in distribution network containing DGs. In *2009 IEEE Region Conference*, Singapore, 23-26 January. DOI:10.1109/TENCON.2009.5396204

[17] Dewadasa, M.; Ghosh, A.; Ledwich, G. and Wishart, M. 2010. Fault isolation in distributed generation connected distribution networks. *IET Generation, Transmission & Distribution 5(10)*:1053-1061.

[18] Jamali, S. and Borhani-Bahabadi, H. 2016. Recloser time current voltage characteristic for fuse saving in distribution networks with DGs. *IET Generation, Transmission & Distribution2017 11(1)*:272-279.

[19] Jamali, S. and Hossien, B. 2017. Self-adaptive relaying scheme of recloser for fuse saving in distribution networks with DGs. *International Journal Power Energy Research 1(1)*:8-19.

[20] Bedekar, P.; Bhidc, S. and Kale, V. 2009. Optimum coordination of overcurrent relay in distribution system using genetic algorithm. In *3rd International Conference on Power Systems*. Kharagpur, India, 27-29 December. DOI: 10.1109/ICPWS.2009.5442716

[21] Ravikumar, V.; Zeineldin, H. H. and Weidong, X. 2013.Determining optimal location and size of distributed generation resources considering Harmonic and Protection Coordination Limits. *IEEE Transection on Power System*,20(2):1245:1254

[22] Khaled, A. S.; Zeineldin H. H.; Al-Hinai, A; and El-Saadany, E.F. 2015. Optimal coordination of Direction relay using a new time current voltage characteristic. 2015, *IEEE Transection on Power Derivery30(2)*:537-544

[23] Khaled, A. S.; Mohamed, S. EI. and Zeineldin H. H.; Al-Hinai, 2015. A new protection scheme considering fault ride through requirement for

transmission level interconnected wind park. *IEEE Transection on Industrial informatics 11(6):*1324-1333

[24] Bayati, N.; Akbar, D.; Sadegh, S.H.H.; Behrooz, V. and Milani, A. E. 2017. Considering variation of network topology in optimal relay coordination using time current voltage characteristic. In *2017 IEEE International Conference on Environment and Electrical Engineering and 2017 IEEE Industrial and Commercial Power Systems Europe*, Milan, Italy, 6-9 June. DOI: 10.1109/EEEIC.2017.7977810

[25] GEC Alsthom. 1987. Protective relays application guide. London: Balding &Mansell.

[26] Benmouyal, G. and G-7 work group. 1999. IEEE standard inverse time characteristic equations for overcurrent relay. *IEEE Transection on Power Derivery14(3):*868-872

[27] Jamali, S. and Hossien, B. 2017. Non-communication protection method for meshed and radial distribution network with synchronous-based DG. *Electrical Power and Energy Systems 93(2017)*:468-478

[28] Anubha, A.; Manohar, S. and Tejeswini M.V. 2016. Voltage current based time inverse relay coordination for PV feed distribution system. *2016 National Power Systems Conference*. Bhubaneswar, India, 19-21 December. DOI: 10.1109/NPSC.2016.7858866

[29] Danilo, L.A.; José C.M.; and Silvio A. 2014. Methodology for modeling overcurrent relays with non-standard curves by using logarithmic-linear correction. In *2014 IEEE PES General Meeting*. National Harbor, MD, USA, 27-31 July.

[30] Hasan, C. K.; Hüseyin, A.; Ibrahim, S. and Bedri, K. 2018. Non-standard characteristic based protection scheme for distribution network. *Energies2018 (11*):1-13.

[31] Kim, T.H.; Kang, S.H.; Seo,W.S. and Kim, M.S. 2015. Voltage-controlled overcurrent relay for a wind farm having looped collection circuits. *2015 IEEE Eindhoven PowerTech*, Eindhoven, Netherlands, 29 Jun-2 July. DOI: 10.1109/PESGM.2014.6939270

[32] Benmouyal, G. and G-7 work group. 1996. IEEE standard inverse time characteristic equations for overcurrent relays (IEEE Std C37.112-1996). The institute of Electrical and Electronics Engineers, New York, USA.